Tea2p Is a Kinesin-like Protein Required to Generate Polarized Growth in Fission Yeast

Heidi Browning,* Jacqueline Hayles,‡ Juan Mata,‡ Lauren Aveline,* Paul Nurse,‡ and J. Richard McIntosh*

*Department of Molecular, Cellular, and Developmental Biology, University of Colorado, Boulder, Colorado, 80309-0347; and ‡Cell Cycle Laboratory, Imperial Cancer Research Fund, London WC2A 3PX, United Kingdom

Abstract. Cytoplasmic microtubules are critical for establishing and maintaining cell shape and polarity. Our investigations of kinesin-like proteins (klps) and morphological mutants in the fission yeast *Schizosaccharomyces pombe* have identified a kinesin-like gene, *tea2*$^+$, that is required for cells to generate proper polarized growth. Cells deleted for this gene are often bent during exponential growth and initiate growth from improper sites as they exit stationary phase. They have a reduced cytoplasmic microtubule network and display severe morphological defects in genetic backgrounds that produce long cells. The tip-specific marker, Tea1p, is mislocalized in both *tea2-1* and *tea2Δ* cells, indicating that Tea2p function is necessary for proper localization of Tea1p. Tea2p is localized to the tips of the cell and in a punctate pattern within the cell, often coincident with the ends of cytoplasmic microtubules. These results suggest that this kinesin promotes microtubule growth, possibly through interactions with the microtubule end, and that it is important for establishing and maintaining polarized growth along the long axis of the cell.

Key words: microtubule • *Schizosaccharomyces pombe* • cytoskeleton • kinesin • cell polarity

Introduction

A particular shape and a well-defined polarity are characteristic of many cell types, as illustrated by the extended morphology of differentiated nerve cells or the asymmetric organization of polarized epithelia. The components of the cytoskeleton play an essential role in establishing and maintaining the morphology of interphase eukaryotic cells (Vasiliev, 1991). The microtubule cytoskeleton participates in this general function by providing an intracellular framework for vesicle transport, by contributing to the internal organization of the cell, and by aiding in the organization and function of the cell cortex.

The interphase microtubule network is generally dynamic, with the addition and loss of tubulin subunits occurring mostly at one microtubule end, the "plus" end (for a review see Desai and Mitchison, 1997), whereas a microtubule's "minus" end is less dynamic and is usually associated with the centrosome or "spindle pole body" (SPB), as it is termed in yeasts. The stability and length of microtubules are governed primarily by the rates of subunit addition and loss and by the frequency of transitions between phases of growth and shrinkage.

Many proteins affect microtubule stability and length, including microtubule-associated proteins (MAPs), kinesin-like proteins (klps),[1] and microtubule-severing enzymes (for a review see Cassimeris, 1999). The klps comprise a superfamily of microtubule-based motor enzymes found in all eukaryotes; they share a conserved motor domain that is responsible for translocation of the enzyme along microtubules. Kinesin itself, the founding member of the superfamily, moves toward the microtubule plus end through the interactions of its NH_2-terminal motor domain (Brady, 1985; Vale et al., 1985), whereas the COOH-terminal or tail region is thought to interact with cargo (Vale and Goldstein, 1990). Additional functions proposed for kinesins include the production of opposing inward and outward forces on the mitotic spindle (for a review see Endow, 1999) and the destabilization of microtu-

Address correspondence to Heidi Browning, 44 Lincoln's Inn Fields, Imperial Cancer Research Fund, London WC2A 3PX, England. Tel.: 44-020-7269-3276. Fax: 44-020-7269-3258. E-mail: browninh@icrf.icnet.uk

H. Browning's present address is Cell Cycle Laboratory, Imperial Cancer Research Fund, London, UK. J. Mata's present address is Developmental Biology Programme, European Molecular Biology Laboratory, Heidelberg, Germany.

[1]*Abbreviations used in this paper:* aa, amino acid(s); cM, centimorgan; DIC, differential interference contrast; EMM, Edinburgh minimal medium; GFP, green fluorescence protein; klp, kinesin-like protein; MBC, methyl 2-benzimidazole-carbonate; ORF, open reading frame; RT-PCR, reverse transcription followed by PCR; TBZ, thiabendazole; YES, yeast extract plus supplements.

Table I. Strains Used in This Study

Strain	Genotype	Source
42	*leu1-32, ura4-D18, ade6-M210, h⁻*	PN557*
99	*his3-D1, leu1-32, ura4-D18, ade6-M210, h⁻*	–
100	*his3-D1, leu1-32, ura4-D18, ade6-M216, h⁺*	–
437	*klp3Δ::ura4⁺, his3-D1, leu1-32, ura4-D18, ade6, h⁺*	This study
438	*tea2Δ::his3⁺, his3-D1, leu1-32, ura4-D18, ade6, h⁺*	This study
439	*klp3Δ::ura4⁺, his3-D1, leu1-32, ura4-D18, ade6, h⁻*	This study
440	*pkl1Δ::his3⁺, klp3Δ::ura4⁺, his3-D1, leu1-32, ura4-D18, ade6*	This study
441	*klp2Δ::ura4⁺, tea2Δ::his3⁺, his3-D1, leu1-32, ura4-D18, ade6, h⁻*	This study
442	*klp2Δ::ura4⁺, his3-D1, leu1-32, ura4-D18, ade6M210, h⁻*	Troxell and McIntosh‡
443	*pkl1Δ::his3⁺, his3-D1, leu1-32, ura4-D18, ade6M216, h⁺*	Pidoux et al., 1996
444	*klp2Δ::ura4⁺, klp3Δ::ura4⁺, his3-D1, leu1-32, ura4-D18, ade6*	This study
445	*klp2Δ::ura4⁺, tea2Δ::his3⁺, klp3Δ::ura4⁺, his3-D1, leu1-32, ura4-D18, ade6*	This study
446	*pkl1Δ::his3⁺, klp3Δ::ura4⁺, tea2Δ::his3⁺, his3-D1, leu1-32, ura4-D18, ade6*	This study
447	*pkl1Δ::his3⁺, klp2Δ::ura4⁺, his3-D1, leu1-32, ura4-D18, ade6M216, h⁻*	This study
448	*pkl1Δ::his3⁺, klp2Δ::ura4⁺, klp3Δ::ura4⁺, his3-D1, leu1-32, ura4-D18, ade6, h⁻*	This study
449	*pkl1Δ::his3⁺, klp2Δ::ura4⁺, tea2Δ::his3⁺, his3-D1, leu1-32, ura4-D18, ade6, h⁻*	This study
451	*tea2Δ::his3⁺, his3-D1, leu1-32, ura4-D18, ade6M210, h⁻*	This study
452	*pkl1Δ::his3⁺, klp2Δ::ura4⁺, klp3Δ::ura4⁺, klp4Δ::his3⁺, his3-D1, leu1-32, ura4-D18, ade6*	This study
453	*pkl1Δ::his3⁺, tea2Δ::his3⁺, his3D1, ura4-D18, ade6, leu1-32*	This study
454	*klp3Δ::ura4⁺, tea2Δ::his3⁺, his3-D1, leu1-32, ura4-D18, ade6, h⁻*	This study
455	*klp3Δ::ura4⁺, tea2Δ::his3⁺, his3-D1, leu1-32, ura4-D18, ade6, h⁺*	This study
PN2466*	*tea2::GFP kan⁺ leu1-32 h⁻*	This study
PN2500*	*tea2::GFP kan⁺ tea1Δ::ura4⁺ ura4-D18*	This study

*PN designations indicate strain from Nurse lab collection.
‡This unpublished strain was provided by C. Troxell and J.R. McIntosh.

bules (Endow et al., 1994; Lombillo et al., 1995a; Lombillo et al., 1995b; Walczak et al., 1996; Desai et al., 1999).

The unicellular fission yeast *Schizosaccharomyces pombe* offers a useful model system in which to study the molecular mechanisms that control eukaryotic cellular morphology because it is amenable to detailed morphological, genetic, and molecular analyses. After cell division, growth begins only at the old end of the cell. Early in G2, growth is also initiated from the new end of the cell (Mitchison and Nurse, 1985), and it continues from both tips until the cell enters mitosis and stops further elongation. Both cytoskeletal and regulatory components that control these events have been identified and characterized (for a review see Snell and Nurse, 1993).

Although the actin cytoskeleton appears to be needed for the actual deposition of growth material (Marks and Hyams, 1985; Kobori et al., 1989; May et al., 1998; Steinberg and McIntosh, 1998), the cytoplasmic microtubule network has been shown in several studies to play a role in defining the site of growth extension (for reviews see Hagan, 1998; Mata and Nurse, 1998). Treatment with a drug that destabilizes microtubules or incubation of temperature-sensitive tubulin mutants at their restrictive temperature results in the formation of branched cells (Toda et al., 1983; Umesono et al., 1983; Radcliffe et al., 1998; Sawin and Nurse, 1998). Genetic screens for mutants with altered polarity have identified mutant alleles of the tubulin genes (Radcliffe et al., 1998) and tubulin-folding cofactors (Hirata et al., 1998; Radcliffe et al., 1999). Moreover, many mutant strains with altered morphology contain abnormal arrays of cytoplasmic microtubules (Verde et al., 1995; Beinhauer et al., 1997; Mata and Nurse, 1997; Hirata et al., 1998; Radcliffe et al., 1998). Cytoplasmic microtubules are also important for the localization of at least two cell tip–specific proteins, Tea1p and Pom1p (Mata and Nurse, 1997; Bahler and Pringle, 1998). Mutations in these genes result in defects in cell morphology and/or bipolar growth (Snell and Nurse, 1994; Verde et al., 1995; Bahler and Pringle, 1998).

We have sought cellular components that work in conjunction with the microtubule cytoskeleton to establish and maintain cellular polarity. Through the molecular identification of *tea2⁺*, a gene identified in a screen for morphology mutants and shown to be required for normal behavior of the cell's growing tip (Verde et al., 1995), we have demonstrated that a klp is required for normal cellular morphology. As described for the mutant alleles of this gene (Verde et al., 1995), the deletion results in defects in the cytoplasmic microtubule array and in cell shape. During the transition out of stationary phase growth, both *tea2Δ* and *tea2-1* cells often establish an ectopic growth site resulting in the formation of T-shaped cells. Likewise, long cells are particularly sensitive to the loss of *tea2⁺*. Tea2p localizes to cell tips and is also often seen as dots coincident with cytoplasmic microtubule ends.

Materials and Methods

Strains and Cell Culture

All strains used are shown in Table I. Strains were constructed and maintained as described in Moreno et al., 1991. Cultures were grown in rich medium containing yeast extract plus supplements (YES) or a Edinburgh minimal medium (EMM; Moreno et al., 1991).

PCR Screen for klps

Primers to conserved portions of the kinesin motor domain were used to amplify genomic DNA. Genomic DNA was prepared as described in Moreno et al., 1991. The 5′ primers were TAC/TGGNCAA/GACNGG

(corresponding toYGQTGSGK) or TAC/TGGNCAA/GACNGG (corresponding to YGQTGTGK), and the 3′ primer was C/TTCNG/CA/TNCCNG (corresponding to DLAGSE). PCR amplifications were performed on three different samples of DNA: (a) genomic DNA from wild-type cells; (b) genomic DNA from wild-type cells digested with XbaI, which restricts within *pkl1* (Pidoux et al., 1996) and *klp2*$^+$; and (c) genomic DNA from *klp2Δ* cells. Reaction conditions were 30 cycles of 95°C for 30 s, 40 or 45°C for 30 s, and 72°C for 30 s, generally followed by a single 5-min incubation at 72°C. PCR products were subcloned and analyzed by colony PCR. To identify clones that represent previously identified klps, colony PCR products were digested with enzymes that cut within *cut7*$^+$ (Hagan and Yanagida, 1990), *pkl1*$^+$, and *klp2*$^+$. Potentially novel products were size-fractionated on low melting point (LMP) agarose to purify the products from PCR primers, and then were sequenced directly in the gel (Kretz et al., 1989, 1990) using vector-specific primers. A total of 163 clones with inserts were analyzed, and two novel kinesin-like genes, designated *klp3*$^+$ and *klp4*$^+$, were identified; *klp3*$^+$ has recently been described by others (Brazer et al., 2000), and will be further characterized elsewhere. *klp4*$^+$ was shown by the work described below to be identical to *tea2*$^+$ (Verde et al., 1995), so that name will be used henceforth.

Cloning of *tea2*$^+$ by Mapping and Complementation

tea2$^+$ was cloned by positional mapping and complementation (Mata and Nurse, 1997). *tea2-1* was mapped to within 0.1 centimorgan (cM) of *orb2ts* (*pak1*$^+$*/shk1*$^+$; Marcus et al., 1995; Ottilie et al., 1995; Verde et al., 1998). The loci were shown to be separate genes by complementation in a *tea2-1*/*orb2ts* heterozygous diploid. The XhoI-BstEII fragment of *pak1*$^+$ was used to probe the Cold Spring Harbor (Mizukami et al., 1993) and Imperial Cancer Research Fund (Hoheisel et al., 1993) cosmid libraries, provided by The Sanger Centre (Cambridge, England). Hybridizing cosmids were tagged with the *his7*$^+$ selectable marker (Morgan et al., 1996) and retransformed into a *tea2-1 his7-36* strain; one cosmid, c1604, was able to rescue the mutant phenotype. This cosmid was used to prepare a SauIIIA partial library in pIRT2 (Hindley et al., 1987), which was transformed into *tea2-1 leu1-32*. Rescuing clones were selected by replica plating to 36°C and examining the cells over the next 2–3 h. *tea2-1* cells normally form a high percentage of T shapes upon regrowth from nutrient starvation. Plasmids were recovered from clones that did not form T shapes under these conditions. Four overlapping clones were obtained, and clone 14T was used for further analyses.

To show that 14T contained *tea2*$^+$ and not an extragenic suppressor, the clone was integrated into the genome by homologous recombination, and this strain was crossed to *leu1-32* and *tea2-1 leu1-32* strains. 14T was mapped to within 0.3 cM of *tea2-1* and the rescuing activity to within 0.5 cM of *LEU2*, demonstrating that the *tea2-1* rescuing activity is linked to 14T and that the site of integration is very close to *tea2-1*.

Molecular Characterization of the *tea2*$^+$ Region

Unless otherwise specified, molecular biology techniques are essentially as described in Sambrook et al., 1989, and sequencing was performed at the University of Colorado automated DNA sequencing facility. A genomic library, provided by A. Carr (Barbet et al., 1992), was screened using the PCR-generated clone of *tea2*$^+$. Of 20,000 clones screened, two unique clones were identified: 11B, which contained a 4.6-kb insert, and a second clone that contained only part of the *tea2*$^+$ open reading frame (ORF). Subclones of 11B were constructed in pSPORT (GIBCO BRL; see Fig. 1 A): the 4.6-kb BamHI (from vector multicloning site) to HindIII fragment was cloned into the BamHI/HindIII sites of pSPORT, creating 11–24; the 2.8-kb BglII fragment spanning the motor domain was inserted into the BamHI site of pSPORT, creating 8–24; and the 1.4-kb AvaI-HindIII fragment was inserted into the AvaI/HindIII sites of pSPORT, creating 4–24. Subclones of 11B were sequenced.

To isolate DNA further 3′ of the *tea2*$^+$ ORF, the 11-kb XhoI fragment extending 3′ from the *tea2*$^+$ ORF was cloned by constructing and screening an XhoI genomic library of 11-kb XhoI genomic fragments cloned into pBluescript. This cloned region, cloneX/X, was digested with XhoI and BamHI, and the 4.3-kb XhoI-BamHI fragment (see Fig. 1 A) was cloned into the XhoI/BamHI sites of pBluescript. This clone, X/B, was used for sequencing and for Northern blot analysis.

A 1.4-kb AvaI/ HindIII fragment containing the 3′ half of *tea2*$^+$ ORF was used to screen a cDNA library (provided by F. LaCroute, Centre de Genetique Moleculare Gif sur Yvette, France). Approximately 60,000 clones were screened, and one cDNA was identified. The cDNA was excised using NotI and were inserted into the NotI site of pSPORT to construct pSPORT*tea2*$^+$ cDNA, and this clone was sequenced.

Total RNA was isolated from wild-type *S. pombe* cells as described in Moreno et al., 1991. Poly(A$^+$) RNA was isolated using GIBCO BRL oligo(dT) cellulose columns according to the manufacturer's recommendations. Northern blot analyses were performed as described in Browning and Strome, 1996. Probes were labeled by random priming using ^{32}P-labeled dATP from Amersham Pharmacia Biotech or NEN Life Science Products.

Reverse transcription followed by PCR (RT-PCR) was performed using the Promega Access RT-PCR kit. Total RNA was used as template with the primer 5′-CGTAGTATATGATTGTAGCAGGTCGTC-3′ for reverse transcription and the primer combination 5′-CGTAGTATATGATTGTAGCAGGTCGTC-3′ and 5′-CTGTGACTCAGGAAACGCAACTTC-3′ for PCR.

Computer-aided Sequence Analysis

The BLAST program available at http://www.ncbi.nlm.nih.gov/BLAST/ was used for sequence searches. The BestFit program from the GCG sequence analysis package was used for direct sequence comparison. For phylogenetic analysis, the ~340–amino acid (aa) motor domains of Tea2p and 42 other klps were aligned using the ClustalW program (Thompson et al., 1994) available at http://dot.imgen.bcm.tmc.edu:9331/multi-align/multi-align.html. This alignment was analyzed with the phylogenetic program PAUP version 4.0 (Sinauer Associates, Inc.), assuming maximum parsimony and using a heuristic search method with stepwise addition. 100 bootstrap replicas were performed. For coiled coil predictions, the Coils program available at http://www.ch.embnet.org/software/COILS_form.html was used (Lupas et al., 1991). Both matrices (MTK and MTIDK) were tested, with and without the weighting option.

Construction of Knockout Strain

A null allele of *tea2*$^+$ was constructed by single-step gene replacement protocol, replacing the *tea2*$^+$ ORF with *his3*$^+$ by homologous recombination. To construct the integration plasmid, clone 11–24 was digested with BbsI, blunt ended with Klenow, then digested with HindIII, and the 423-bp [BbsI]-HindIII fragment beginning 14 bp 3′ of *tea2*$^+$ ORF was isolated. A SalI/SmaI fragment containing *his3*$^+$ was isolated from pAFI (Ohi et al., 1996). These two fragments were simultaneously ligated into the SalI and HindIII sites in pSPORT to create an intermediate integration construct. To place *tea2*$^+$ 5′ flanking DNA into this plasmid, clone 8–24 was digested with PflmI, DNA ends were blunt ended with T4 DNA polymerase, the plasmid was further digested with KpnI, and the fragment from KpnI (in the vector multicloning site) to [PflmI], which contains the *tea2*$^+$ 5′ flanking DNA, was ligated into the KpnI/SmaI sites of the intermediate integration construct. The final integration plasmid contained 1,063 bp of 5′ and 423 bp of 3′ DNA from the region flanking the *tea2*$^+$ ORF placed on the 5′ and 3′ sides of *his3*$^+$, respectively. For transformation, the *tea2-his3*$^+$ cassette was excised by digestion with PvuII. Diploids (*his3-D1/his3-D1, ura4-D18/ura4-D18, ade6-M210/ade6-M216, leu1-32/leu1-32*, h$^+$/h$^-$) were transformed with this cassette using the PLATE method (Elble, 1992). Homologous integrants were identified by PCR and confirmed by Southern blot analysis.

Identification of *tea2*$^+$ and *klp4*$^+$ as the Same Gene

The gene initially characterized as *klp4*$^+$ was found to be entirely contained within the 14T plasmid using PCR primers specific to *klp4*$^+$. Clone 14T was used to construct 5′ and 3′ deletions to further define the rescuing region (see Fig. 1 A). 14B and 14H are 3′ truncations with deletions extending to the BamHI and HindIII sites, respectively. 14X is a deletion with 5′ sequences removed to the XhoI site. The *tea2-1* allele was sequenced by PCR amplification of *tea2-1* genomic DNA using primers specific to the *tea2*$^+$ region followed by sequencing of the PCR products.

Inducing Cells to Exit from Stationary Phase

Cells were grown in YES or EMM at 32°C until they reached stationary phase growth, generally 1 d beyond logarithmic growth in YES or 2 d after logarithmic growth in EMM. Cells were then diluted 1:10 or 1:25 in fresh medium and examined by microscopy at various times after dilution. For *tea2Δ* complementation tests, cells were grown to saturation in EMM with appropriate supplements. For lineage analysis, cells were grown to saturation in YES, placed on a YES agar pad (YES medium with 2% agar) on a microscope slide, and examined by differential interference contrast

(DIC) microscopy using a Zeiss microscope. The slide was warmed to 32°C with an air curtain incubator (Sage Instruments) or a heatlamp. The temperature was controlled using a CN76000 microprocessor-based temperature and process controller from Omega Engineering. Images were captured using an Empix charge-coupled device camera and Metamorph software (Universal Imaging).

Production of Antibodies

For protein expression in *Escherichia coli*, a construct was made by digestion of clone 4–24 with BsmI and BbsI and generation of blunt ends with T4 DNA polymerase and Klenow. The 440-bp [BsmI-BbsI] fragment corresponding to the COOH-terminal region of Tea2p (which lacks motor sequences) was cloned into the EcoRI site of pGEXKG (Guan and Dixon, 1991), which had been blunt ended with Klenow. Inclusion bodies were purified from cells expressing this construct, pGEXKG*tea2*s/t, by the method of Lin and Cheng, 1991. The fusion protein was further purified by SDS-PAGE. Fusion protein was electroeluted from the gel, dialyzed against 1X PBS, and sent to Strategic Biosolutions for the immunization of two rabbits.

A second fusion protein was constructed for antibody purification. The 440-bp [BsmI-BbsI] *tea2*$^+$ fragment described above was cloned into the PvuII site of pRSETc (Invitrogen) and the fusion protein expressed in the BL21(DE3) *E. coli* strain. The fusion protein was solubilized by denaturization and then purified by chromatography on nickel columns according to the procedure recommended by Invitrogen. A column for affinity purification was made with purified fusion protein covalently cross-linked to cyanogen bromide–activated sepharose 4B (Sigma-Aldrich) as recommended by Amersham Pharmacia Biotech. The serum was purified on the column essentially as described in Harlow and Lane (1988), except 1× PBS was substituted for 10 mM Tris (pH 7.5 and 8.8), and the unbound antibody was washed off the column with 5 bed volumes 1× PBS, 10 bed volumes 3× PBS, and 15 bed volumes 1× PBS.

Immunofluorescence Microscopy

Cells were prepared for immunofluorescence staining by aldehyde or cold methanol fixation as described in Hagan and Hyams, 1988. For tubulin staining, a mouse moncolonal antibody against *Drosophila* α-tubulin was used (provided by M.T. Fuller, Stanford University, Stanford, CA) or tat1 (Woods et al., 1989; a gift from Keith Gull, University of Manchester, Manchester, UK) with goat anti–mouse Alexa secondary antibody (Molecular Probes). Tea2p–green fluorescence protein (GFP) was visualized using a rabbit polyclonal antibody at 1:200 (a gift from Ken Sawin, Imperial Cancer Research Fund, London, UK) and Alexa 488 (Molecular Probes) as the secondary antibody. For Tea2p antibody staining, secondary antibodies were fluorescein-labeled goat anti–rabbit immunoglobulin (Jackson ImmunoResearch Laboratories). Tea1p staining was as described in Mata and Nurse, 1997. Tea2p staining was performed on methanol-fixed cells. Cells were mounted in Citifluor Mountant Media No. 0 (Ted Pella, Inc.).

Immunofluorescence microscopy was performed on a Leica DMRXA/RF4/V automated universal microscope, and images were acquired with a Cooke SensiCam high performance digital camera using the Slidebook software package (Intelligent Imaging Innovations, Inc.) or a Zeiss LSM510 Confocal microscope. In all cases, images were exported to Adobe Photoshop for figure preparation.

Immunoblot Analysis

pREP3X*tea2*$^+$ cDNA was constructed by cloning the BamHI/SmaI 4.6-kb fragment from pSPORT*tea2*$^+$cDNA into the BamH1 and SmaI sites of pREP3X (Maundrell, 1993). The truncated cDNA construct was made by digesting pREP3X*tea2*$^+$ cDNA with BbsI, filling in the 5′ overhang with Klenow, and then digesting with BamHI. The BamHI/[BbsI] fragment containing the entire ORF of *tea2*$^+$ was then cloned into the SmaI and BamHI sites of pREP3X. *tea2Δ* cells transformed with these constructs were grown in EMM with appropriate supplements and 5 μg/ml thiamine (Sigma-Aldrich), and cells were washed three times with thiamine-free medium then grown overnight in thiamine-free medium. Cells were harvested, and protein extracts prepared by vortexing cells with glass beads in sample buffer.

Western blot analysis was performed as described in Towbin et al. (1979). 4% nonfat dry milk was used as a blocking agent. Blots were developed using enhanced chemiluminescence (ECL) reagents from Amersham Pharmacia Biotech.

Construction of Tea2-GFP Homologous Integration Strain

Tea2 was tagged with GFP at the COOH terminus as described in Bahler et al. (1998) using the forward primer 5′GAAACTAAAACTGAAATTTTGCCAGACGATCAACAGCAATCGAAAAAGGATTCTGTGACTCAGGAAACGCAACTTCTTTCTCGGATCCCCGGGTTAATTAA 3′ and the reverse primer 3′AATTTAAGGAGACATACAGGTTGAATGGGTATAAAATTGTAAACAAGGTTGATGAGAGACGCCTATAATTAAACAAGGTAGAATTCGAGCTCGTTTAAAC 3′. 1–2 μg of PCR product was transformed into *ade6-M210/216 leu1-32/1-32 h*$^+$*/h*$^+$ cells and G418-resistant clones were selected and then sporulated. G418-resistant haploids were screened by PCR for homologous integration at the *tea2*$^+$ locus. The morphology of one strain was tested upon recovery from nutrient starvation and in exponential growth. The strain was also tested for Tea1p localization and microtubule length. In all conditions tested, the Tea2p-GFP–tagged strain behaved as wild-type cells.

Results

Isolation of the Kinesin-like Gene, tea2$^+$, by PCR and Phenotype Rescue

To understand the roles of klps in *S. pombe*, we carried out a PCR screen using degenerate primers to highly conserved regions in the motor domain of the kinesin superfamily. Two new *S. pombe* klps were identified, *klp3*$^+$ (to be discussed elsewhere and Brazer et al., 2000) and *klp4*$^+$. The PCR-generated clone for *klp4*$^+$ was used to identify a genomic clone, 11B, containing the *klp4*$^+$ ORF (Fig. 1 A), and a fragment of this genomic region was used to identify a cDNA clone (Fig. 1 A). Sequence analysis revealed that the 4583-bp cDNA contained the entire *klp4*$^+$ ORF with a stop codon at the same position as predicted from the genomic sequence, as well as 2.6 kb of additional 3′ sequence that unexpectedly contained a second ORF of 658 aa (Fig. 1 A). A fragment containing the downstream genomic region was cloned, clone X/X, and both this clone and clone 14T (described below) were used to sequence the genomic region corresponding to the cDNA clone (Fig. 1 A). Comparison of the genomic and cDNA sequences indicated that there are no introns in *klp4*$^+$.

The PCR-generated clone also was used to map *klp4*$^+$ by hybridization to a cosmid filter of the *S. pombe* genome (Hoheisel et al., 1993) to chromosome 2 between *puc1*$^+$ and *nda3*$^+$. This region has since been sequenced by the *S. pombe* Sanger Centre genome project, and is located on cosmid c1604 with EMBL/GenBank/DDBJ accession nos. AL034433 and PID g4376084.

In an independent, parallel series of experiments, we were investigating the localization of Tea1p in *tea2-1* cells and found that Tea1p was mostly delocalized from the cell tips compared with wild-type cells and was found along the microtubules and in the cytoplasm (data not shown). This result suggests that Tea2p might be required to transport Tea1p to the cell tips. To investigate this possibility, *tea2*$^+$ was mapped by positional cloning to cosmid c1604 (described in Materials and Methods). This cosmid was subcloned, and the 14T plasmid, a subclone capable of rescuing the *tea2-1* morphology defects, was used for further analyses.

The similarity of the phenotypes of the knockout of *klp4*$^+$ (described below) and mutant alleles of *tea2*$^+$ (Verde et al., 1995), together with the mapping data described above and in Materials and Methods, suggested

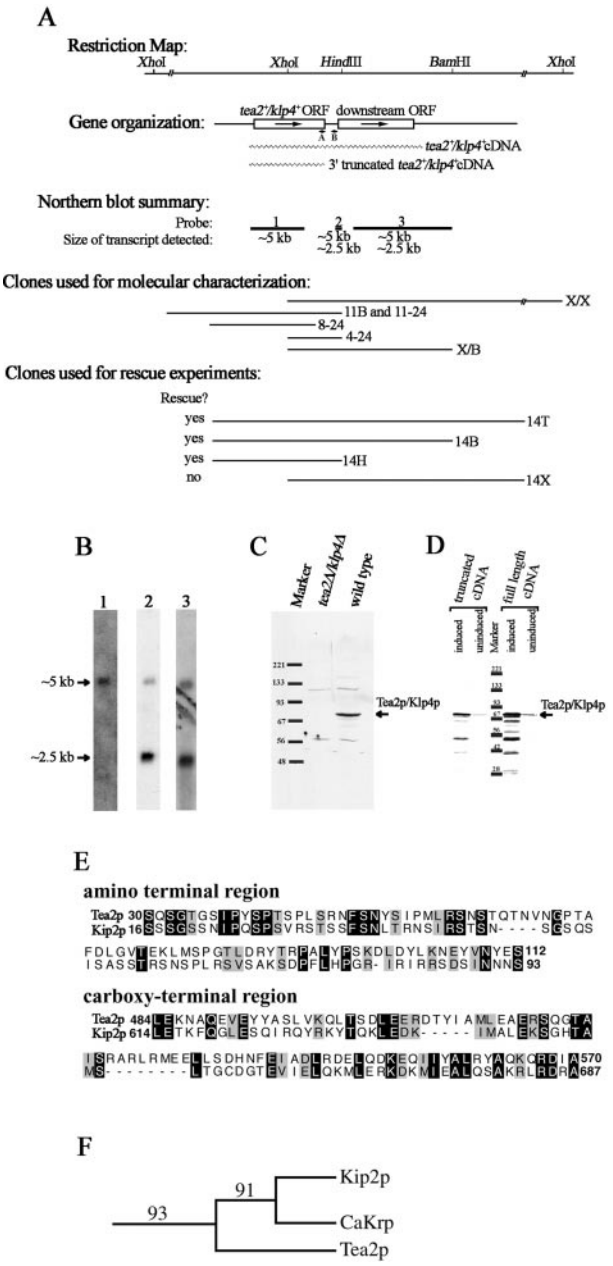

Figure 1. Molecular analysis of *tea2*$^+$. (A) Schematic representation of the *tea2*$^+$ genomic region. The top section is a restriction map (additional HindIII and BamHI sites not shown). The second section illustrates the gene organization with a schematic representation of the ORFs. Arrows indicate the direction of transcription and wavy lines represent the cDNA clones used in D. The short lines labeled A and B represent the location of the primers used for RT-PCR, which is described in the text. The third section is a summary of the results from the Northern blot analysis shown in B. Lines designated 1, 2, and 3 represent coverage of probes used for the Northern blot analysis, with the size of the transcript detected for each probe written under the line. The fourth section illustrates the clones used for molecular analysis, which are described in the text. Section five shows clones used for rescue experiments. All sections are aligned with the restriction map. (B) Transcriptional analysis of the *tea2*$^+$ region. Probes designated 1, 2, and 3 in A were hybridized to polyA$^+$ RNA isolated from wild-type cells. (C) Western blot analysis. Protein extracts were obtained from *tea2Δ* and wild-type cells in logarithmic growth. The blot was reacted with antibodies to Tea2p. The upper and lower background bands appear with variable intensities from blot to blot. (D) Western blot analysis of cDNA transformants. For expression of the full-length and truncated cDNAs, cells transformed with pREP3X*tea2*$^+$cDNA and pREP3X*tea2*$^+$ORF were used. The blot was reacted with antibodies to Tea2p. (E) Sequence alignment. Nonmotor regions of Tea2p and Kip2p were aligned using BestFit and displayed using BOXSHADE. Identical aa are highlighted in black, and similar aa are highlighted in grey. (F) Bootstrap analysis. The branch structure shows the Kip2p subfamily of the kinesin superfamily. The numbers illustrate bootstrap values for 100 replicas.

Table II. Rescue of tea2Δ Exit from Stationary Phase Phenotype

Strain	T- or L-shaped cells before dilution	T- or L-shaped cells 2.5 h after dilution
	%	%
14T transformed *tea2Δ* cells (11 clones*)	<1 (2/1758)	<1 (5/2078)
14B transformed *tea2Δ* cells (3 clones tested*)	<1 (1/426)	<1 (3/430)
14H transformed *tea2Δ* cells (3 clones tested*)	0 (0/427)	<1 (2/427)
14X transformed *tea2Δ* cells (3 clones tested*)	<1 (1/338)	23 (95/416)
IRT2 transformed *tea2Δ* cells (7 clones tested*)	<1 (6/1396)	21 (246/1178)
Untransformed *tea2Δ* cells	<1 (0/110)	19 (26/135)

Cells were grown to stationary phase at 32°C, diluted into fresh medium, and then allowed to exit stationary phase at 32°C.
*At least 100 cells counted for each clone.

that these two independently identified genes might be the same genetic locus. To explore this possibility, three sets of PCR primers covering the *klp4*$^+$ region were used to amplify DNA from the 14T plasmid, and all three gave bands of the expected size, indicating that the 14T plasmid contained the entire *klp4*$^+$ ORF. Transformation of the 14T plasmid into a strain deleted for *klp4*$^+$ (described below) resulted in rescue of the *klp4Δ* phenotype (Table II), and the plasmids 14B and 14H (Fig. 1 A) also rescued both the *klp4Δ* phenotype (Table II) and the *tea2-1* phenotype. However, neither the deletion nor the *tea2-1* mutant was rescued by the 5′ truncation construct, 14X, that lacks 896 bp of the *klp4*$^+$ ORF but leaves the downstream ORF intact (Fig. 1 A). The 14T plasmid was also integrated into the genome, and the site of integration was genetically mapped to the *tea2*$^+$ locus (described in Materials and Methods). In addition, the region corresponding to the *klp4*$^+$ ORF was sequenced in DNA isolated from *tea2-1* cells and shown to have a serine to phenylalanine transition at aa 384. This serine residue is in the motor domain and is a highly conserved aa found in nearly all klps.

These results establish that *tea2*$^+$ and *klp4*$^+$ encode the same gene; from this point on, the gene will be referred to as *tea2*$^+$ and its protein product as Tea2p.

Characterization of the tea2$^+$ *Transcript and Protein Product*

Sequence analysis of the genomic and cDNA clones indicated that *tea2*$^+$ potentially encodes a 628-aa protein that

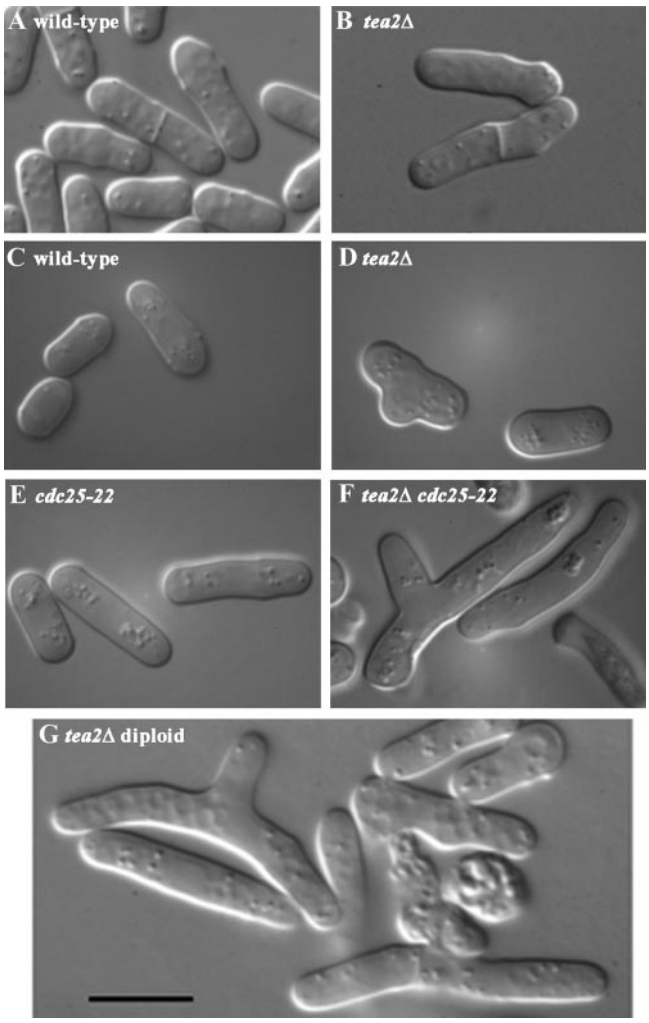

Figure 2. DIC microscopy of (A) wild-type and (B) *tea2Δ* cells grown to mid-log phase. DIC microscopy of (C) wild-type, (D) *tea2Δ*, (E) *cdc25-22*, and (F) *tea2Δ cdc25-22* cells from colonies on plates and (G) *tea2Δ* diploid cells from liquid culture. Bar: 10 μm.

is expressed from a transcript of at least 4.6 kb and that contains 2.6 kb of 3′ sequence. This 3′ region contains a second ORF of 658 aa (accession nos. AL034433 and PID g4007771). Because this is an unusual structure for an *S. pombe* gene, we sought additional evidence for the gene structure of *tea2*$^+$. The region corresponding to the *tea2*$^+$ ORF hybridized to a ~5-kb transcript on Northern blots (Fig. 1 B, probe 1). Northern blot analyses using probes further 3′ indicate that the ~5-kb *tea2*$^+$ transcript extends in this direction, and that a second transcript of 2.5 kb is present in this region (Fig. 1 B, probes 2 and 3). This smaller transcript presumably codes for the ORF in this region that is predicted from the genomic sequence.

The junction between the two ORFs was confirmed by RT-PCR performed on RNA from wild-type cells. Primer B (Fig. 1 A) at the predicted 5′ end of the downstream gene was used for the reverse transcriptase reaction, and this primer in combination with primer A corresponding to the 3′ end of the *tea2*$^+$ ORF was used for PCR. An RT-PCR product of 315 nucleotides was produced, indicating that this region is uninterrupted by introns (not shown).

Analysis of the protein product further supports the proposed genomic structure of the region. Affinity-purified antibodies generated to the COOH-terminal region of Tea2p reacted with an ~70-kD protein in wild-type cells, which was absent in cells deleted for the *tea2*$^+$ ORF (Fig. 1 C). Furthermore, *tea2Δ* cells expressing just the *tea2*$^+$ ORF or the entire *tea2*$^+$ cDNA under the control of the inducible *nmt*$^+$ promoter produced a protein of the expected size for Tea2p (Fig. 1 D).

Finally, the 2.6-kb 3′ region of the *tea2*$^+$ transcript is not essential for rescue of the mutant phenotype. A multicopy plasmid containing the *tea2*$^+$ ORF, 14H, rescued the phenotype of both *tea2Δ* and *tea2-1* cells (Fig. 1 A; Table II).

Sequence Comparison Analysis

Sequence searches using the motor domain of Tea2p revealed that of all the klps that have been characterized (beyond mere identification in a genome project), it is most similar to *Saccharomyces cerevisiae* Kip2p. Direct comparison of the motor domains, using the BestFit program from the GCG sequence analysis package, demonstrated that Tea2p and Kip2p are 58% similar and 51% identical over 332 aa. The motor domains of both proteins lie roughly in the middle of the proteins: the Kip2p motor domain extends from residues 97 to 500 within the 706-aa protein, and the Tea2p motor domain runs from residues 129 to 467 within the 628-aa protein. Outside the motor domain, the sequences are 35% similar and 26% identical over an 83-aa stretch in the NH_2-terminal region and 46% similar and 32% identical over an 87-aa stretch in the COOH-terminal region (Fig. 1 E). In the COOH terminus, Tea2p is predicted to contain one or two coiled coil regions of 28–41 aa, depending on the matrix employed and whether the weighting option was used (Lupas et al., 1991). Kip2p also contains regions in the COOH terminus predicted to form a coiled coil, suggesting that both these motors are capable of self-association.

An alignment containing Tea2p, Kip2p, and 41 other kinesin family members was analyzed with the phylogenetic program PAUP (version 4.0), assuming maximum parsimony and using a heuristic search method with stepwise addition (described in Materials and Methods). This analysis revealed that of 100 bootstrap replicas, 93 grouped Kip2p, Tea2p, and CaKrp together (Fig. 1 F; CaKrp is a klp identified by the *Candida albicans* genome project). A value of >90 strongly supports a phylogenetic relationship on statistical grounds (Goodson et al., 1994). These klps represent a new subfamily, which we will refer to as the Kip2p subfamily after its founding member.

Defects in Cell Morphology and in the Microtubule Cytoskeleton

To investigate further the cellular roles of Tea2p in *S. pombe*, a deletion allele was constructed by replacing the *tea2*$^+$ ORF with *his3*$^+$. Transformants were screened by PCR, and homologous integration was confirmed by Southern blot analysis (not shown). At 32°C, *tea2Δ* cells grow at rates similar to wild-type cells. These cells were examined by DIC microscopy to see if the deletion had an effect on the morphology of the cells. Cultures of exponentially growing cells contain ~18% (n = 117) obviously

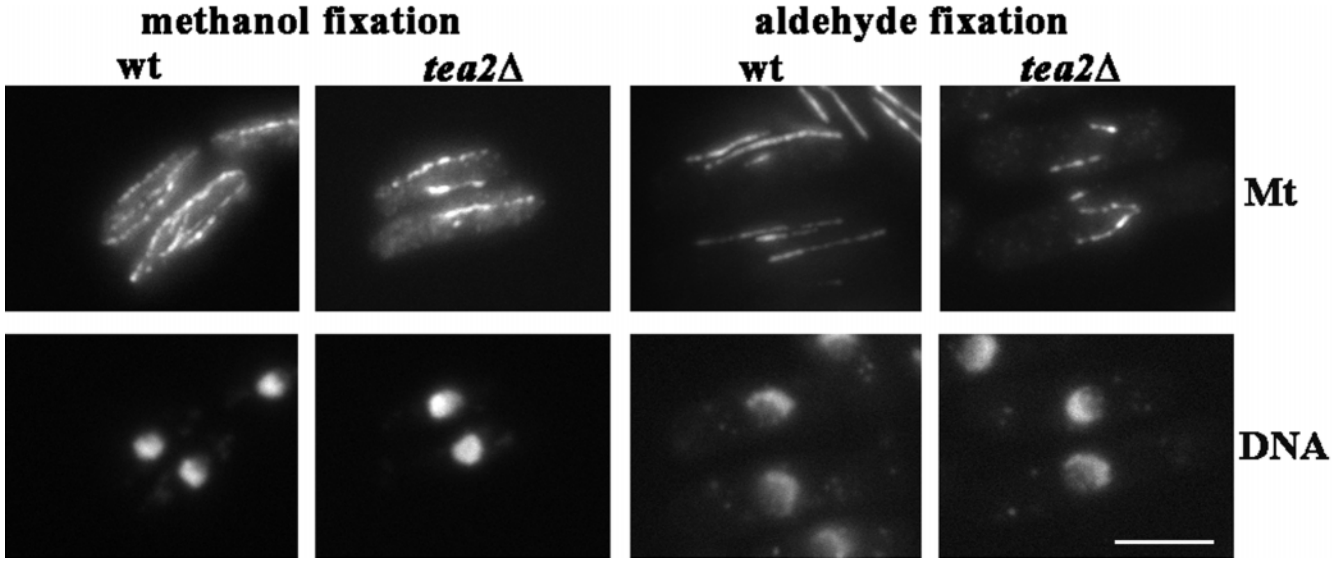

Figure 3. Microtubule staining (Mt) of wild-type and *tea2Δ* cells grown to mid-log phase and then fixed with methanol or aldehyde and stained with tubulin antibody and DAPI (DNA). Microtubule images are the projection of serial optical sections encompassing the entire depth of the cell. Bar: 5 μm.

bent cells, whereas wild-type cells were generally straight cylinders, 0% bent (n = 138; Fig. 2, A and B). At 37°C, *tea2Δ* cells grew more slowly than wild-type cells, and a high percentage of T shaped cells were seen in the culture (up to 9%). These defects in cell morphology are similar to the *tea2-1* mutant (Verde et al., 1995).

Because defects in cell shape may be related to defects in the cytoskeleton and because *tea2* mutant alleles have short cytoplasmic microtubules (Verde et al., 1995), we examined the microtubule cytoskeleton in *tea2Δ* cells (Fig. 3). Exponentially growing cells were stained with antibodies to tubulin, and the cytoplasmic microtubule network was found to be severely reduced (Fig. 3). The defects appeared to be more severe when the cells were fixed with aldehyde rather than methanol, perhaps because of a difference in microtubule stability that is reflected by sensitivity to fixation. Astral microtubules were examined in *tea2Δ* cells using a tubulin-gfp construct (Ding et al., 1998), and were found to be much shorter than those seen in wild-type cells (data not shown).

It seemed possible that a transition from a phase of nongrowth to a phase of growth might involve an extensive reestablishment of cell polarity and therefore necessitate a relocalization of tip-defining components. This possibility was supported by an observation made during the cloning of *tea2*$^+$: *tea2-1* cells had a more severe phenotype upon recovery from nutrient starvation. In addition, colonies of *tea2Δ* cells had variable percentages of T-shaped cells, perhaps caused by nutrient variations in the colony (Fig. 2 D). To investigate these observations in more detail, we examined polarity reestablishment in *tea2Δ* cells as they emerged from stationary phase at 32°C. After *tea2Δ* cells were grown to saturation in liquid rich medium and then diluted into fresh medium, 75% (n = 700) acquired a T-shaped morphology. (Hundreds of wild-type cells examined all maintained their cylindical shape upon exit from stationary phase.) To more fully examine this defect in *tea2Δ* cells, 107 individual cells were followed by DIC microscopy through the first few divisions after release from stationary phase (Fig. 4). 63 of the cells developed a T shape, 7 developed an L shape, and 6 developed other abnormal morphologies, whereas 31 developed relatively normally. T-shaped cells were tracked through their second division, and 36/39 of these cells grew again from the same ectopic site in the next division (Fig. 4). In contrast, 34/34 of the normal shaped cells produced from the first division of the T-shaped cells underwent a normal subsequent division (Fig. 4). This lineage analysis suggests that upon exit from stationary phase, a cell that intiates growth from an ectopic site generally continues to use that ectopic site in the subsequent division. Furthermore, once a cell acquires a nonbranched morphology (i.e., the daughter cell formed from the base of the T), this cell is able to maintain a relatively normal morphology in the following divisions. This latter point is further supported by the ab-

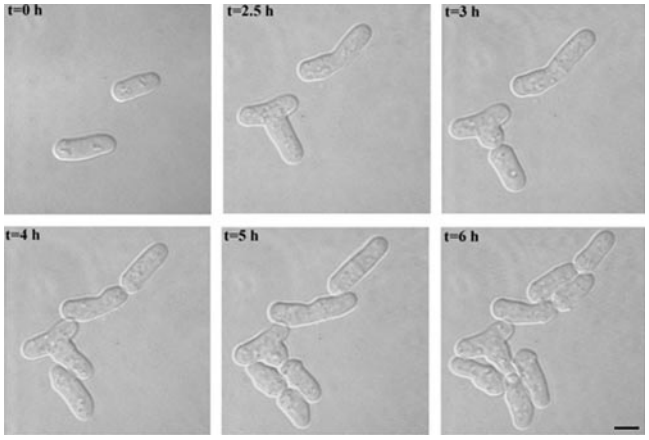

Figure 4. DIC microscopy of the first and second division out of stationary phase of *tea2Δ* cells. Cells were grown to saturation in YES medium, placed on a YES agar pad, and examined at the indicated times as the cells exited stationary phase. (Bar: 5 μm).

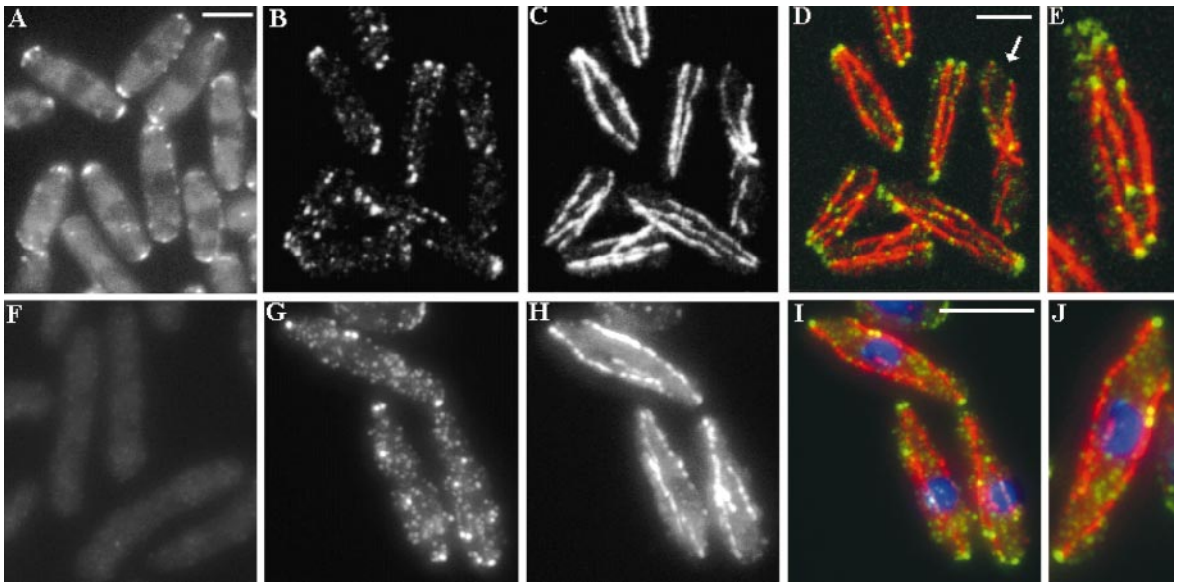

Figure 5. Localization of Tea2p in logarithmic phase cells. (A) Tea2-GFP viewed in live cells. (B–E) *tea2-GFP* cells fixed and stained with antibodies to (B) GFP, (C) tubulin, (D) merged image, and (E) enlarged, merged image. (D) Cell with arrow has just completed anaphase as exhibited by the postanaphase array of microtubules. (F) *tea2Δ* cells fixed and stained with antibodies to Tea2p. Wild-type cells fixed and stained with antibodies to (G) Tea2p, (H) tubulin, (I) merged image, and (J) enlarged, merged image. Bar in D corresponds to images B–D; bar in I corresponds to images F–I. Bar: 5 μm.

sence of T-shaped cells in exponentially growing cultures at 32°C.

Enhancement of Morphological Defects with Increases in Cell Length

The short cytoplasmic microtubules in *tea2Δ* cells were generally clustered around the nucleus. This arrangement of the cytoskeleton might be especially detrimental in long cells because they may require a more extensive microtubule transport system for tip specification. To test this idea, the phenotype of *tea2Δ* in genetic backgrounds that result in long cells was examined. Entry into mitosis is delayed in *cdc25-22* cells even at permissive temperature, so these cells are 54% longer than wild-type cells at the time of division (Fantes, 1979). *tea2Δ cdc25-22* cells grown at permissive temperature formed microcolonies of very long and often branched cells (Fig. 2, C–F), indicating that the extra length of *cdc25-22* cells cannot be tolerated in a *tea2Δ* background. This interpretation was supported by similar observations in diploid cells, which are 85% longer than haploid cells (Nurse and Thuriaux, 1980). Homozygous diploid *tea2Δ* cells grew poorly; they are very unstable, haploidize at a high frequency, and are often bent or branched (Fig. 2 G).

Examination of Essential Functions among klps

To investigate redundancy for essential functions of *tea2*$^+$ and other klps, double, triple, and quadruple mutants were constructed with *pkl1Δ* (Pidoux et al., 1996), *klp2Δ* (C. Troxell and J.R. McIntosh, personal communication), *klp3Δ* (described in Materials and Methods and in Brazer et al., 2000), and *tea2Δ*. All possible mutant combinations were constructed. Deletions were monitored by the auxotrophic markers used to delete each gene and by colony PCR using primers specific for each deletion. All combinations were viable at 32°C. To test for temperature sensitivity, each strain was streaked on a YES agar plate and grown at 32°C. These plates were replica plated to EMM agar with appropriate supplements and YES agar plates, and were incubated at 20°C, 25°C, 32°C, and 35.5°C. All mutant combinations were able to grow at these temperatures, suggesting that there are no redundancies of essential functions between Tea2p and these other klps.

Localization of Tea2p

The cellular localization of Tea2p was determined by fusing the endogenous *tea2*$^+$ at its 3′ end with the gene for GFP by homologous recombination. Exponentially growing cells were examined by epifluorescence microscopy, and Tea2p-GFP was seen concentrated at the cell tips with some fluorescence throughout the cytoplasm, particularly as cytoplasmic dots (Fig. 5 A). Because the fluorescence from Tea2p-GFP was faint, some cells were fixed and stained with antibodies to GFP in an effort to enhance the signal (Fig. 5, B–E). As in live cells, Tea2p-GFP was seen at the cell tips, but the signal to noise ratio of the overall cytoplasmic pattern was enhanced in fixed cells. Punctate staining throughout the cytoplasm was observed in these cells. This is likely to be a combined result of signal enhancement, due to the use of antibodies, and some delocalization caused by fixation. Costaining with antibodies to GFP and microtubules revealed that the most intense cytoplasmic dots generally colocalized with the interphase microtubules and were sometimes at the microtubules' ends (Fig. 5, B–E). In mitotic cells, Tea2p-GFP was less concentrated at the cell tips (Fig. 5 D, cell with arrow).

The localization of the GFP tagged allele was confirmed using antibodies generated against a fusion protein containing GST and the stalk/tail region of Tea2p. The resulting immune sera were affinity purified against a second fu-

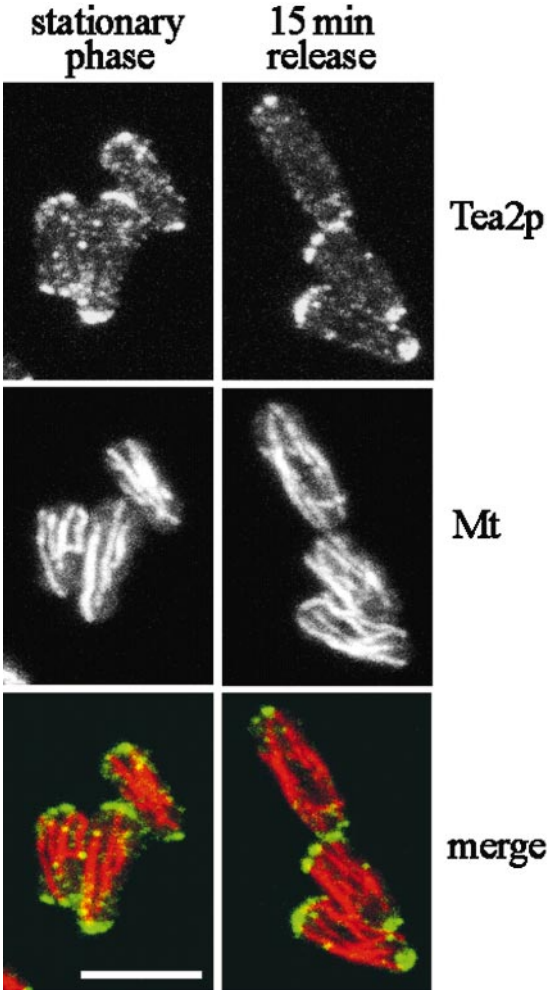

Figure 6. Localization of Tea2p in stationary phase cells and in cells exiting stationary phase. Wild-type cells were grown to stationary phase and then fixed and stained with antibodies to Tea2p (Tea2p) and tubulin (Mt), or were diluted into fresh medium, grown 15 min, and then fixed and stained. Images are the projection of serial optical sections encompassing the entire depth of the cell. Bar: 5 μm.

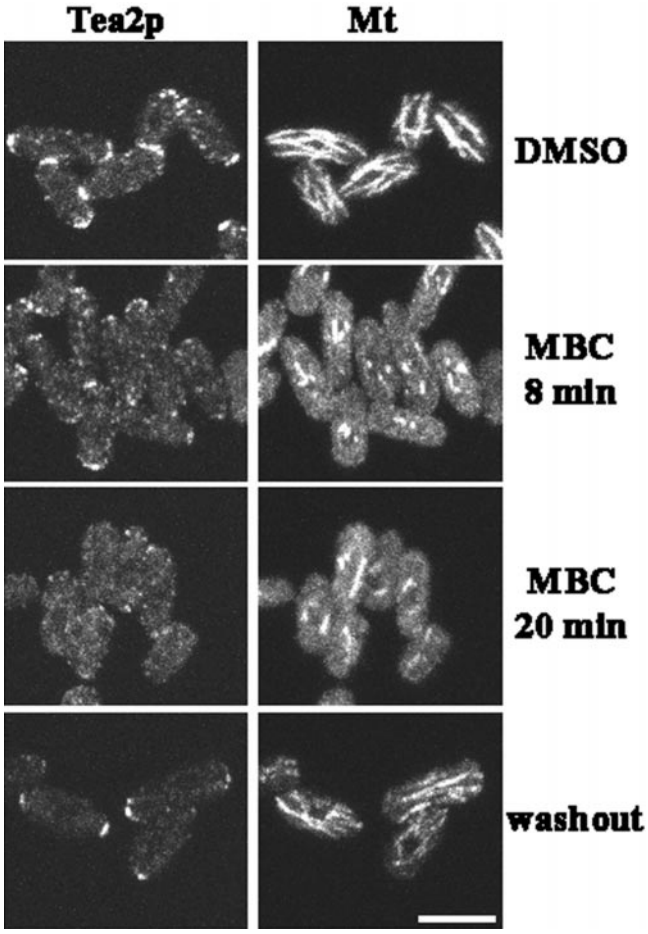

Figure 7. Dependence of Tea2p on microtubules for localization. Cells exiting stationary phase were treated with DMSO (control) or MBC dissolved in DMSO, and then were fixed and stained with antibodies to Tea2p (Tea2p) and tubulin (Mt). MBC was washed out (washout), and the cells were allowed to recover for 18 min, then were fixed and stained. Bar: 5 μm.

sion protein that contained the Tea2p stalk/tail region tagged with six histidines, and the purified antibodies were used to examine the localization of Tea2p in exponentially growing cells. Staining of *tea2Δ* cells showed very faint cytoplasmic background fluorescence (Fig. 5 F). In exponentially growing wild-type cells, Tea2p was detected at the cell tips and often at the end of cytoplasmic microtubules (Fig. 5, G–J), whereas in mitotic cells Tea2p was less concentrated at the cell tips (not shown).

Because of the severity of the morphological defects observed as cells emerged from stationary phase, the localization of Tea2p was examined in stationary phase cells and in cells as they were released from growth arrest. In fixed cells, Tea2p was more concentrated at the cell tips in stationary phase cells and in cells released from stationary phase than in exponentially growing cultures (Fig. 6). This could be a reflection of increased resistance to delocalization by fixation, as well as to a change in distribution. Both in stationary phase and in cells exiting stationary phase, non–cell tip staining was often found to be coincident with microtubules or microtubule ends (Fig. 6).

Tea2p Dependence on Microtubules for Localization

To determine whether microtubules are required for Tea2p localization, the position of Tea2p was determined in the presence of the microtubule poison methyl 2-benzimidazolecarbamate (MBC). Because Tea2p is concentrated at the cell tips in cells exiting from stationary phase, this transition was used to characterize the need for microtubules for Tea2p tip localization. Wild-type cells were grown to stationary phase, diluted into fresh medium, and allowed to grow for 25 min. MBC (25 μg/ml) or DMSO (control cells) was then added to the culture, and the cells were further incubated with aliquots removed at 5, 8, and 20 min for staining with antibodies to Tea2p and microtubules. Although the cytoplasmic microtubule network was severely reduced at the 5- and 8-min time points, Tea2p remained concentrated at the cell tips (Fig. 7; 8-min time point shown). By 20 min, Tea2p was no longer concentrated at the cell tips, but after the drug was washed out and the microtubules were allowed to repolymerize,

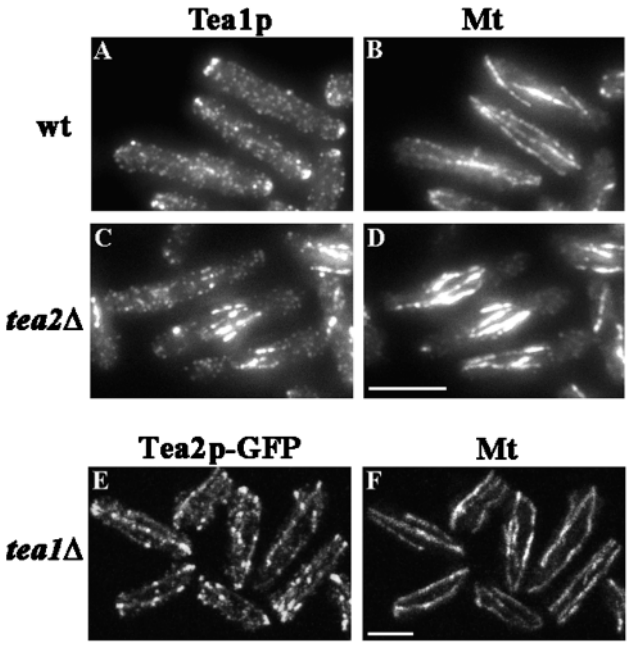

Figure 8. Tea1p localization in *tea2Δ* cells, and Tea2p-GFP localization in *tea1Δ*. (A and B) Wild-type and (C and D) *tea2Δ* cells were grown to logarithmic phase, and then were fixed and stained with antibodies to (A and C) Tea1p and (B and D) tubulin. *tea1Δ tea2-GFP* cells were stained with antibodies to (E) GFP or (F) tubulin. Bar in D corresponds to A–D; bar in F corresponds to E and F. Bar: 5 μm.

Tea2p relocalized to the cell tips (Fig. 7). These results suggest that microtubules are required for transporting Tea2p to the tip but not for the short-term maintenance of this localization. Treatment with the microtubule poison thiabendazole (TBZ) or cold shock also resulted in the delocalization of Tea2p (data not shown).

Localization of Tea1p in tea2-1 and tea2Δ Cells and Tea2p in tea1Δ Cells

Tea1p is proposed to be an end marker that directs the growth machinery to the cell tip (Mata and Nurse, 1997). It localizes to the cell tips throughout the cell cycle, and this localization is dependent on microtubules. To investigate the possible role of Tea2p in the localization of Tea1p, exponentially growing *tea2-1*, *tea2Δ*, and wild-type cells were stained with antibodies to Tea1p (Fig. 8, A–D; wild-type and *tea2Δ* cells shown). In wild-type cells, Tea1p localized to the cell tips (Fig. 8 A; Mata and Nurse, 1997), whereas in the *tea2-1* and *tea2Δ* mutant cells, Tea1p localized primarily to the short cytoplasmic microtubules (Fig. 8, C and D; *tea2Δ* shown). Finally, to investigate whether Tea1p had an effect on Tea2p localization, we examined the localization of Tea2p-GFP in a *tea1Δ* strain. Tea2p-GFP was still localized at the cell tips, but was more extended in distribution along the microtubules compared with a wild-type strain (compare Fig. 8, E and F, with Fig. 5).

Discussion

Tea2p Affects Cellular Morphology through an Interaction with Microtubules

We have shown that *tea2*$^+$ encodes a klp that is required to establish proper cellular morphology in the fission yeast. Mutant alleles of *tea2*$^+$ (Verde et al., 1995), including its complete deletion, result in cytoplasmic microtubules of reduced length. Because microtubules are required for proper cellular morphology in *S. pombe*, the abnormal microtubule cytoskeleton is likely to contribute to the morphological abnormalities observed in *tea2Δ* cells. These shape abnormalities are most severe in long cells, either diploids or mutants that are longer than haploid wild-type cells, and in cells progressing from a phase of nongrowth to a phase of growth. These results suggest that the importance of microtubules for normal cell growth varies with cell length and growth stage. Tea2p localizes to the cell tips and often to the ends of cytoplasmic microtubules including microtubules that do not reach the cell tip; its localization at cell tips is dependent on cytoplasmic microtubules. Analysis of microtubule dynamics in wild-type cells suggests that microtubules extend from the cell center out to the cell tips, with the minus ends located near the nucleus and the plus ends at the cell tips (Drummond and Cross, 2000). Microtubules seen in fixed cells to extend from cell tip to tip probably represent two interphase arrays with minus ends overlapping near the cell equator (Drummond and Cross, 2000). Thus, the localization of Tea2p at the cell tips suggests that, if this kinesin has motor activity, it is plus end directed.

The localization of Tea2p and the phenotype of *tea2Δ* and *tea2-1* mutants are consistent with two mechanisms by which Tea2p might function: Tea2p may affect the length of microtubules through a direct interaction with the microtubules, or it could act indirectly by transporting one or more proteins to the plus end of microtubules, which in turn results in microtubule stabilization. In either case, because there is a high concentration of microtubule plus ends at the cell tips (Hagan and Hyams, 1988; Drummond and Cross, 2000), the concentration of Tea2p at the cell tips supports the hypothesis that the Tea2p-mediated stabilization of microtubules is occurring at the plus ends of the microtubules.

In the first model, Tea2p could act directly on the end of a microtubule to affect the rate of polymerization or depolymerization, or the frequency of rescue or catastrophy. Previous analyses have revealed that klps can affect the dynamic stability of microtubules in vitro (Endow et al., 1994; Lombillo et al., 1995a; Lombillo et al., 1995b; Walczak et al., 1996, 1997; Desai et al., 1999). For example, Kar3p, a klp from *S. cerevisiae*, induces depolymerization from microtubule minus ends in vitro (Endow et al., 1994), and XKCM1 and XKIF2 from Xenopus destabilize both microtubule ends in vitro (Desai et al., 1999). Several microtubule-based motor proteins affect the lengths of the spindle and/or cytoplasmic microtubules of *S. cerevisiae* in vivo: deletion of *KAR3*, *DYN1*, or *KIP3* results in longer cytoplasmic microtubules or spindles, whereas deletion or mutation of *KIP2*, *CIN8*, or *KIP1* result in shorter cytoplasmic microtubules or spindles (Cottingham and Hoyt,

1997; Saunders et al., 1997a,b; Huyett et al., 1998; Miller et al., 1998).

In the second model, Tea2p would bind tip-specific protein(s) and transport them along microtubules to their plus ends. The cargo proteins could then modulate microtubule stability, promoting growth. As the microtubules elongate, by either the direct or indirect mechanism, they would be expected to reach the cell tip; interaction there with the cell cortex could provide additional regulation of the length and stability of the microtubule. Kirschner and Mitchison (1986) proposed a similar model to explain the reorganization of the microtubule cytoskeleton observed during polarization of various cell types. They suggested that the asymmetric reorganization of the microtubule cytoskeleton could be controlled at the cell periphery by a localized stabilization of the microtubule ends. Cortical complexes that interact with microtubules have been described previously. For example, in several organisms, alignment of the mitotic spindle is thought to occur through an interaction of the astral microtubules and the cell cortex, resulting in the rotation or movement of the centrosome–nuclear complex or mitotic spindle toward the cortical site (Lutz et al., 1988; Dan and Tanaka, 1990; Allen and Kropf, 1992; White and Strome, 1996; Heil-Chapdelaine et al., 1999). In *S. cerevisiae*, capture of astral microtubules at the cortical site appears to occur through an interaction between the EB1 homologue Bim1p and the cortical marker protein Kar9p (Korinek et al., 2000; Lee et al., 2000).

Comparison of Tea2p with S. cerevisiae klps

The analyses of klps in *S. cerevisiae* have provided a wealth of information about the roles of these enzymes in cell behavior, but none of the mutations in budding yeast has the effect described here for the deletion of *tea2*$^+$ in fission yeast. This is likely to be due to the observation that *S. cerevisiae*, in contrast to *S. pombe*, does not require cytoplasmic microtubules for morphological decisions and development (Jacobs et al., 1988). Instead, microtubules and microtubule motors are required for the proper positioning of the nucleus, spindle formation and function, mating, and karyogamy (reviewed in Stearns, 1997; Marsh and Rose, 1997). Tea2p is most similar in sequence to the *S. cerevisiae* Kip2p and to a klp identified by the *Candida albicans* genome project. Phylogenetic analysis illustrates that these enzymes represent a new subfamily of klps. Although deletion of *KIP2* also results in short cytoplasmic microtubules, the consequence is a defect in nuclear migration rather than a change in cellular morphology (Cottingham and Hoyt, 1997; Huyett et al., 1998; Miller et al., 1998). This difference in phenotypic effect could be a result of the different functions of cytoplasmic microtubules in these two yeasts rather than a divergence in the role of the related klps.

Possible Cargoes of Tea2p: Tea1p Requires Tea2p for Proper Localization

Tea2p may also transport proteins that help to define the cell's growing tip. Several proteins that are important for cell morphology are also localized to the cell tip including Tea1p and Pom1p (Mata and Nurse, 1997; Bahler and Pringle, 1998). These two proteins are candidates for cargoes of Tea2p because disruption of microtubules disrupts their localization (Mata and Nurse, 1997; Bahler and Pringle, 1998). Pom1p is a protein kinase required for the reinitiation of growth from the old end of the cell after cytokinesis, the switch to bipolar growth, and the positioning of the septum (Bahler and Pringle, 1998). The microtubule network in *pom1Δ* cells appears normal (Bahler and Pringle, 1998), so this protein is more likely to be part of a tip-defining complex rather a microtubule-regulating complex.

Tea1p has been proposed to direct the cell growth machinery to the cell tip (Mata and Nurse, 1997). Tea1p localizes to the cell tips throughout the cell cycle, and its localization is dependent on microtubules. In the absence of Tea1p, 30–35% of cells are obviously bent during phases of growth, suggesting that this protein is required for normal antipodal growth. Cells deleted for *tea1*$^+$ can have unusually long cytoplasmic microtubules that curl around the end of the cell in 10–15% of the cells versus $<0.5\%$ in wild-type cells (Mata and Nurse, 1997). This microtubule phenotype supports the hypothesis that Tea1p is part of a microtubule-controlling complex.

In the absence of Tea2p, Tea1p localizes along the short cytoplasmic microtubules characteristic of *tea2Δ* cells. Therefore, although Tea1p has an affinity for microtubules in the absence of Tea2p, proper localization of Tea1p to the cell tip requires Tea2p. One possibility is that Tea2p transports Tea1p along microtubules and deposits it at the cell tip. A second possibility is that Tea1p uses another microtubule-mediated mechanism to get to the tip of the cell, and the absence of a normal array of cytoplasmic microtubules in *tea2Δ* cells results in the mislocalization of Tea1p.

Tea1p may also have a direct effect on Tea2p localization. When *tea1*$^+$ is deleted, Tea2p is distributed more broadly along the microtubules, possibly because it is moving more slowly or binding to microtubules less efficiently. Alternatively, Tea1p may be required for efficient anchoring of Tea2p to the cell tip. Interestingly, although both proteins require microtubules for tip-specific localization, they are able to remain at the cell tips for short periods in the absence of microtubules, suggesting that the requirement for microtubules is for transport but not for anchorage (Fig. 7; Mata and Nurse, 1997).

Our analyses of Tea2p and *tea2* mutant cells provide new evidence for the role of microtubules in the proper positioning of the growth site in fission yeast. The involvement of the microtubule cytoskeleton in the control of cell shape is a widely observed phenomenon that is likely to have many conserved components. Determining whether the mechanism by which Tea2p functions is through the direct stabilization of microtubules or the transport of a microtubule-regulating complex will provide insight into the control of morphogenesis in *S. pombe*, and this mechanism may represent a more general function of klps in the morphology of eukaryotic cells.

The authors wish to thank Robert West, Ken Sawin, Takashi Toda, Paula Grissom, Katya Grishchuk, Cynthia Troxell, Alison Pidoux, Zac Cande, and Damian Brunner for plasmids, antibodies, strains, helpful suggestions, and critical reading of the manuscript. We thank Mark Winey for the gen-

erous use of his microscope, which was sponsored in part by Virginia and Mel Clark. We are grateful to Scott Kelley for help with the phylogenetic analysis. Yuming Han in the University of Colorado automated sequencing facility sequenced the *tea2*$^+$ clones.

This work was supported by National Institutes of Health (NIH) grant GM-36663 to J.R. McIntosh and by the Imperial Cancer Research Fund. H. Browning was supported in part by NIH postdoctoral fellowship GM-17117 and by a postdoctoral fellowship from the International Agency for Research on Cancer.

Submitted: 27 March 2000
Revised: 16 August 2000
Accepted: 17 August 2000

References

Allen, V.W., and D.L. Kropf. 1992. Nuclear rotation and lineage specification in *Pelvetia* embryos. *Development.* 115:873–883.

Bahler, J., and J. Pringle. 1998. Pom1p, a fission yeast protein kinase that provides positional information for both polarized growth and cytokinesis. *Genes Dev.* 12:1356–1370.

Bahler, J., J.-Q. Wu, M.S. Longtine, N.G. Shah, A. McKenzie III, A.B. Steever, A. Wach, P. Philippsen, and J.R. Pringle. 1998. Heterologous modules for efficient and versatile PCR-based gene targeting in *Schizosaccharomyces pombe*. *Yeast.* 14:943–951.

Barbet, N., W.J. Muriel, and A.M. Carr. 1992. Versatile shuttle vectors and genomic libraries for use with *Schizosaccharomyces pombe*. *Gene.* 114:59–66.

Beinhauer, J., I. Hagan, J. Hegemann, and U. Fleig. 1997. Mal3, the fission yeast homologue of the human APC-interacting protein EB-1 is required for microtubule integrity and the maintenance of cell form. *J. Cell Biol.* 139:717–728.

Brady, S.T. 1985. A novel brain ATPase with properties expected for the fast axonal transport motor. *Nature.* 317:73–75

Brazer, S.C., H.P. Williams, T.G. Chappell, and W.Z. Cande. 2000. A fission yeast kinesin affects Golgi membrane recycling. *Yeast*. 16:149–166

Browning, H., and S. Strome. 1996. A sperm-supplied factor required for embryogenesis in *C. elegans*. *Development.* 122:391–404.

Cassimeris, L. 1999. Accessory protein regulation of microtubule dynamics throughout the cell cycle. *Curr. Opin. Cell Biol.* 11:134–141.

Cottingham, F., and M.A. Hoyt. 1997. Mitotic spindle positioning in *Saccharomyces cerevisiae* is accomplished by antagonistically acting microtubule motor proteins. *J. Cell Biol.* 138:1041–1053.

Dan, K., and Y. Tanaka. 1990. Attachment of one spindle pole to the cortex in unequal cleavage. *Ann. NY Acad. Sci.* 582:108–119.

Desai, A., and T.J. Mitchison. 1997. Microtubule polymerization dynamics. *Annu. Rev. Cell Dev. Biol.* 13:83–117.

Desai, A., S. Verma, J. Mitchison, and C. Walczak. 1999. Kin I kinesins are microtubule-destabilizing enzymes. *Cell*. 96:69–78.

Ding, D.Q., Y. Chikashige, T. Haraguchi, and Y. Hiraoka. 1998. Oscillatory nuclear movement in fission yeast meiotic prophase is driven by astral microtubules, as revealed by continuous observation of chromosomes and microtubules in living cells. *J. Cell Sci.* 111:701–712.

Drummond, D.R., and R.A. Cross. 2000. Dynamics of interphase microtubules in *Schizosaccharomyces pombe*. *Curr. Biol.* 10:766–775.

Elble, R. 1992. A simple and efficient procedure for transformation of yeasts. *Biotechniques.* 13:18–20.

Endow, S.A. 1999. Microtubule motors in spindle and chromosome motility. *Eur. J. Biochem.* 262:12–18.

Endow, S., S. Kang, L. Satterwhite, M. Rose, V. Skeen, and E. Salmon. 1994. Yeast Kar3 is a minus-end microtubule motor protein that destablizes microtubules preferentially at the minus ends. *EMBO (Eur. Mol. Biol. Organ.) J.* 13:2708–2713.

Fantes, P. 1979. Epistatic gene interactions in the control of division in fission yeast. *Nature.* 279:428–430.

Goodson, H.V., S.J. Kang, and S.A. Endow. 1994. Molecular phylogeny of the kinesin family of microtubule motor proteins. *J. Cell Sci.* 107:1875–1884.

Guan, K.L., and J.E. Dixon. 1991. Eukaryotic proteins expressed in *Escherichia coli*: an improved thrombin cleavage and purification procedure of fusion proteins with glutathione *S*-transferase. *Anal. Biochem.* 192:262–267.

Hagan, I.M. 1998. The fission yeast microtubule cytoskeleton. *J. Cell Sci.* 111: 1603–1612.

Hagan, I., and J. Hyams. 1988. The use of cell division cycle mutants to investigate the control of microtubule distribution in the fission yeast *Schizosaccharomyces pombe*. *J. Cell Sci.* 89:343–356.

Hagan, I., and M. Yanagida. 1990. Novel potential mitotic motor protein encoded by the fission yeast *cut7*$^+$ gene. *Nature.* 347:563–566.

Harlow, E., and D. Lane. 1988. Antibodies: A Laboratory Manual. Cold Spring Harbor Laboratory Press, Cold Spring Harbor, NY. 726 pp.

Heil-Chapdelaine, R.A., N.R. Adames, and J.A. Cooper. 1999. Formin' the connection between microtubules and the cell cortex. *J. Cell Biol.* 144:809–811

Hindley J., G. Phear, M. Stein, and D. Beach. 1987. *Sucl*$^+$ encodes a predicted 13-kilodalton protein that is essential for cell viability and is directly involved in the division cycle of *Schizosaccharomyces pombe*. *Mol. Cell. Biol.* 7:504–511.

Hirata, D., H. Masuda, M. Eddison, and T. Toda. 1998. Essential role of tubulin-folding cofactor D in microtubule assembly and its association with microtubules in fission yeast. *EMBO (Eur. Mol. Biol. Organ.) J.* 17:658–666.

Hoheisel, J.D., E. Maier, R. Mott, L. McCarthy, A.V. Grigoriev, L.C. Schalkwyk, D. Nizetic, F. Francis, and H. Lehrach. 1993. High-resolution cosmid and P1-maps spanning the 14MB genome of the fission yeast *S. pombe*. *Cell.* 73:109–120.

Huyett, A., J. Kahana, P. Silver, X. Zeng, and W.S. Saunders. 1998. The Kar3p and Kip2p motors function antagonistically at the spindle poles to influence cytoplasmic microtubule numbers. *J. Cell Sci.* 111:295–301.

Jacobs, C.W., A.E. Adams, P.J. Szaniszlo, and J.R. Pringle. 1988. Functions of microtubules in the *Saccharomyces cerevisiae* cell cycle. *J. Cell Biol.* 107: 1409–1426.

Kirschner, M., and T. Mitchison. 1986. Beyond self-assembly: from microtubules to morphogenesis. *Cell.* 45:329–342.

Kobori, H., N. Yamada, A. Taki, and M. Osumi. 1989. Actin is associated with the formation of the cell wall in reverting protoplasts of the fission yeast *Schizosaccharomyces pombe*. *J. Cell Sci.* 94:635–646.

Korinek, W.S., M.J. Copeland, A. Chaudhuri, J. Chant. 2000. Molecular linkage underlying microtubule orientation toward cortical sites in yeast. *Science.* 287:2257–2259.

Kretz, K.A., G.S. Carson, and J.S. O'Brien. 1989. Direct sequencing from low-melt agarose with Sequenase. *Nucleic Acids Res.* 17:5864.

Kretz, K.A., G.S. Carson, and J.S. O'Brien. 1990. Direct sequencing from low-melt agarose with Sequenase. *Nucleic Acids Res.* 18:400.

Lee, L., J.S. Tirnauer, J. Li, S.C. Schuyler, J.Y. Liu, and D. Pellman. 2000. Positioning of the mitotic spindle by a cortical-microtubule capture mechanism. *Science.* 287:2260–2262.

Lin, K., and S. Cheng. 1991. An efficient method to purify active eukaryotic proteins from the inclusion bodies in *Escherichia coli*. *Biotechniques.* 11:748–752.

Lombillo, V., C. Nislow, T. Yen, V. Gelfand, and J.R. McIntosh. 1995a. Antibodies to the kinesin motor domain and CENP-E inhibit microtubule depolymerization-dependent motion of chromosomes in vitro. *J. Cell Biol.* 128: 107–115.

Lombillo V.A., R.J. Stewart, and J.R. McIntosh. 1995b. Minus-end-directed motion of kinesin-coated microspheres driven by microtubule depolymerization. *Nature.* 373:161–164.

Lupas, A., M. Van Dyke, and J. Stock. 1991. Predicting coiled coils from protein sequences. *Science.* 252:1162–1164.

Lutz, D.A., Y. Hamaguchi, and S. Inoue. 1988. Micromainpulation studies of the asymmetric positioning of the maturation spindle in *Chaetopterus sp.* oocytes: I. Anchorage of the spindle to the cortex and migration of a displaced spindle. *Cell Motil. Cytoskelet.* 11:83–96.

Marcus, S., A. Polverino, E. Chang, D. Robbins, M.H. Cobb, and M.H. Wigler. 1995. Shk1, a homolog of the *Saccharomyces cerevisiae* Ste20 and mammalian p65PAK protein kinase, is a component of a Ras/Cdc42 signaling module in the fission yeast *Schizosaccharomyces pombe*. *Proc. Natl. Acad. Sci. USA*. 92:6180–6184.

Marks, J., and J.S. Hyams. 1985. Localization of F-actin through the cell division cycle of Schizosaccharomyces pombe. *Eur. J. Cell Biol.* 39:27–32.

Marsh, L., and M. Rose. 1997. The pathway of cell and nuclear fusion during mating in *S. cerevisiae*. *In* The Molecular and Cellular Biology of the Yeast Saccharomyces. J.R. Pringle, J.R. Broach, and E.W. Jones, editors. Cold Spring Harbor Laboratory Press, Cold Spring Harbor, NY. 827–888.

Mata, J., and P. Nurse. 1997. tea1 and the microtubule cytoskeleton are important for generating global spatial order within the fission yeast cell. *Cell.* 89: 939–949.

Mata, J., and P. Nurse. 1998. Discovering the poles in yeast. *Trends Cell Biol.* 8:163–167.

Maundrell, K. 1993. Thiamine-repressible expression vectors pREP and pRIP for fission yeast. *Gene.* 123:127–130.

May, K.M., S.P. Wheatley, V. Amin, and J.S. Hyams. 1998. The myosin ATPase inhibitor 2,3-butanedione-2-monoxime (BDM) inhibits tip growth and cytokinesis in the fission yeast, *Schizosaccharomycees pombe*. *Cell Motil. Cytoskel.* 41:117–125.

Miller, R.K., K.K. Heller, L. Frisen, D.L. Wallack, D. Loayza, A.E. Gammie, M.D. Rose. 1998. The kinesin-related proteins, Kip2p and Kip3p, function differently in nuclear migration in yeast. *Mol. Biol. Cell.* 9:2051–2068.

Mitchison, J.M., and P. Nurse. 1985. Growth in cell length in the fission yeast *Schizosaccharomyces pombe*. *J. Cell Sci.* 75:357–376.

Mizukami, T., W.I. Chang, I. Garkavtsev, N. Kaplan, D. Lombardi, T. Matsumot, O. Niwa, A. Kounosu, M. Yanigida, T. G. Marr, and D. Beach. 1993. A 13 kb resolution cosmid map of the 14 Mb fission yeast genome by nonrandom sequence-tagged site mapping. *Cell.* 73:121–132.

Moreno, S., A. Klar, and P. Nurse. 1991. Molecular genetic analysis of fission yeast *Schizosaccharomyces pombe*. *Methods Enzymol.* 194:795–823.

Morgan, B.A., F.L. Conlon, M. Manzanares, J.B.A. Millar, N. Kanuga, J. Sharpe, R. Krumlauf, J.C. Smith, and S.G. Sedgwick. 1996. Transposon tools for recombinant DNA manipulation: characterization of transcriptional regulators from yeast, Xenopus and mouse. *Proc. Natl. Acad. Sci. USA*. 93: 2801–2806.

Nurse, P., and P. Thuriaux. 1980. Regulatory genes controlling mitosis in the fission yeast *Schizosaccharomyces pombe*. *Genetics.* 96:627–637.

Ohi, R., A. Feoktistova, and K.L. Gould. 1996. Construction of vectors and a genomic library for use with *his3*-deficient strains of *Schizosaccharomyces pombe*. *Gene.* 174:315–318.

Ottilie, S., P.J. Miller, D.I. Johnson, C.L. Creasy, M.A. Sells, S. Bagrodia, S.L. Forsburg, and J. Chernoff. 1995. Fission yeast *pak1*$^+$ encodes a protein kinase that interacts with Cdc42p and is involved in the control of cell polarity and mating. *EMBO (Eur. Mol. Biol. Organ.) J.* 14:5908–5919.

Pidoux, A.L., M. LeDizet, and W.Z. Cande. 1996. Fission yeast pkl1 is a kinesin-related protein involved in mitotic spindle function. *Mol. Biol. Cell.* 7:1639–1655.

Radcliffe, P., D. Hirata, D. Childs, L. Vardy, and T. Toda. 1998. Identification of novel temperature-sensitive lethal alleles in essential beta-tubulin and nonessential alpha 2-tubulin genes as fission yeast polarity mutants. *Mol. Biol. Cell.* 9:1757–1771.

Radcliffe, P., D. Hirata, L. Vardy, and T. Toda. 1999. Functional dissection and hierarchy of tubulin-folding cofactor homologues in fission yeast. *Mol. Biol. Cell.* 10:2987–3001.

Sambrook, J., E.F. Fritsch, and T. Maniatis. 1989. Molecular Cloning: A Laboratory Manual. 2nd ed. Cold Spring Harbor Laboratory Press, Cold Spring Harbor, New York.

Saunders W., V. Lengyel, and M.A. Hoyt. 1997a. Mitotic spindle function in *Saccharomyces cerevisiae* requires a balance between different types of kinesin-related motors. *Mol. Biol. Cell.* 8:1025–1033.

Saunders, W., D. Hornack, V. Lengyel, and C. Deng. 1997b. The *Saccharomyces cerevisiae* kinesin-related motor Kar3p acts at preanaphase spindle poles to limit the number and length of cytoplasmic microtubules. *J. Cell Biol.* 137: 417–431.

Sawin, K., and P. Nurse. 1998. Regulation of cell polarity by microtubules in fission yeast. *J. Cell Biol.* 142:457–471.

Snell, V., and P. Nurse. 1993. Investigations into the control of cell form and polarity: the use of morphological mutants in fission yeast. *Dev. Suppl.* 289–299.

Snell, V., and P. Nurse. 1994. Genetic analysis of cell morphogenesis in fission yeast-a role for casein kinase II in the establishment of polarized growth. *EMBO (Eur. Mol. Biol. Organ.) J.* 13:2066–2074.

Stearns, T. 1997. Motoring to a finish: kinesin and dynein work together to orient the mitotic spindle. *J. Cell Biol.* 138:957–960.

Steinberg, G., and J.R. McIntosh. 1998. Effects of the myosin inhibitor 2,3-butanedione monoxime on the physiology of fission yeast. *Eur. J. Cell Biol.* 77:284–293.

Thompson, J.D., D.G. Higgins, and T.J. Gibson. 1994. CLUSTAL W: improving the sensitivity of progressive multiple sequence alignment through sequence weighting, positions-specific gap penalties and weight matrix choice. *Nucleic Acids Res.* 22:4673–4680.

Toda, T., K. Umesono, A. Hirata, and M. Yanagida. 1983. Cold-sensitive nuclear division arrest mutants of the fission yeast *Schizosaccharomyces pombe*. *J. Mol. Biol.* 168:251–270.

Towbin, H., T. Staehelin, and J. Gordon. 1979. Electrophoretic transfer of proteins from polyacrylamide gels to nitrocellulose sheets: procedure and some applications. *Proc. Natl. Acad. Sci. USA*. 76:4350–4354.

Umesono K., T. Toda, S. Hayashi, and M. Yanagida. 1983. Cell division cycle genes *nda2* and *nda3* of the fission yeast *Schizosaccharomyces pombe* control microtubular organization and sensitivity to anti-mitotic benzimidazole compounds. *J. Mol. Biol.* 168:271–284.

Vale, R.D., T.S. Reese, and M.P. Sheetz. 1985. Identification of a novel force-generating protein, kinesin, involved in microtubule-based motility. *Cell.* 42: 39–50.

Vale, R.D., and L.S.B. Goldstein. 1990. One motor, many tails: an expanding repertoire of force-generating enzymes. *Cell.* 60:883–885.

Vasiliev, J.M. 1991. Polarization of pseudopodial activities: cytosketal mechanisms. *J. Cell Sci.* 98:1–4.

Verde, F., J. Mata, and P. Nurse. 1995. Fission yeast cell morphogenesis: identification of new genes and analysis of their role during the cell cycle. *J. Cell Biol.* 131:1529–1538.

Verde, F., D.J. Wiley, and P. Nurse. 1998. Fission yeast *orb6*, a ser/thr protein kinase related to the mammalian rho kinase and myotonic dystrophy kinase, is required for the maintenance of cell polarity and coordinates cell morphogenesis with the cell cycle. *Proc. Natl. Acad. Sci. USA*. 95:7526–7531.

Walczak, C., T. Mitchison, and A. Desai. 1996. XKCM1: a Xenopus kinesin-related protein that regulates microtubule dynamics during spindle assembly. *Cell*. 84:37–47.

Walczak, C., S. Verma, and T. Mitchison. 1997. XCTK2: a kinesin-related protein that promotes mitotic spindle assembly in *Xenopus laevis* egg extracts. *J. Cell Biol.* 136:859–870.

White, J., and S. Strome. 1996. Cleavage plane specification in *C. elegans*: how to divide the spoils. *Cell*. 84:195–198.

Woods, A., T. Sherwin, R. Sasse, T. McRae, A. Baines, and K. Gull. 1989. Definition of individual components within the cytoskeleton of *Trypanosoma brucei* by a library of monoclonal antibodies. *J. Cell Sci.* 93:491–500.